Nonlinear Free Vibration Analysis of Non-uniform Axially Graded Beam on Variable Elastic Foundation

Hareram Lohar
Assistant Professor
Jadavpur University
Department of Mechanical Engineering
India

Anirban Mitra
Associate Professor
Jadavpur University
Department of Mechanical Engineering
India

The present work investigates the nonlinear free vibration of an axially functionally graded (AFG) beam supported on the variable foundation. The beam geometry is non-uniform, with a linear cross-section variation along the length. The beam material is graded along the axial direction following the power-law relation. A Winkler type of variable elastic foundation is taken, in which variation of stiffness is considered along the length of the foundation. Geometrical nonlinearity produced by the beam's large-amplitude deflection is also considered. To attain the desired objectives, the problem is divided into two parts. The static problem is solved first, then a subsequent free vibration analysis is executed on the statically deformed beam configuration. The governing differential equations of the system are derived using suitable energy methods. A numerical technique of direct substitution with relaxation is utilized to obtain the solution of the derived nonlinear differential equations. A suitable validation study is presented to ensure the appropriateness of the present methodology. Benchmark results are also presented by means of natural frequency, backbone curve, and mode shape plot to investigate the influences of elastic foundation, material gradation, and non-uniform geometry on nonlinear vibration.

Keywords: *Nonlinear vibration, AFG beam, Variable elastic foundation, Energy principle.*

1. INTRODUCTION

Modern technology needs sophisticated advanced mate–rials to fulfill the demand of civilization. Functionally graded materials (FGM) fall in this advanced materials category in which smooth and functional transition of material properties is possible to obtain suitable volume fraction. Traditional homogeneous and isotropic materials cannot meet practical needs as they lack the refinement of material property distribution. The main advantages of FG materials are high strength, lightweight, and heat resistance. Koizumi [1] in detail investigated the characteristics and material properties of FGMs. FGMs are one kind of composite material with a microscopic inhomogeneous character [2]. Un–like traditional composite, FGM does not suffer from the problem of delamination, which is caused due to high-stress concentration at the interface of two layers of dissimilar materials [3-6]. On the other hand, the foundation's structure plays an important role in engineering. It has extensive applications in road, railroad, bio-mechanics, geotechnics, and marine engi–neering to design highway pavement, railroad tracks, and continuously supported pipelines, buildings, flo–ating decks, etc. [7]. Its applications in various engi–neering problems have attracted researchers over the years. Its journey can be traced from the year 1867 to the classical textbook by Emil Winkler. In which a simplified model was proposed. At a later time, the effort was extended by several researchers to develop various foundation models. Various researchers throughout the years extensively explore FG beams on elastic foundations.

Pradhan and Murmu [8] presented a thermo-mechanical formulation and utilized the principle of differential quadrature approach to carry out a compa–rative study to analyze the dynamic characteristics of FG sandwich beam. Attar et al. [9] modeled a cracked beam using the lattice spring technique to calculate the beam's natural frequencies. Yaghoobi and Torabi [10] performed a vibration and stability study of FG beams. Mohanty et al [11] presented a FEM model to study the buckling of thick FG and FG sandwich beams. Murin et al. [12] considered the axial force effect on FGM beams to study the free vibrational behavior of the beam. Mohanty et al [13] conducted stability analysis on a la–yered non-uniform beam subjected to the action axially varying load. The prediction of natural frequency and nonlinear frequency response behavior of FG beam was carried out by Kanani et al. [14]. Cubic nonlinearity for the beam was taken into account. Niknam and Aghdam [15] presented a quasi-analytical approach to determine the loaded frequency and critical buckling behavior of FG nonlocal beams. Tossapanon and Wattanasakulpong [16] used the Chebyshev collocation technique to predict vibrational frequencies and buckling load of FG sandwich beam. Deng et al. [17] predicted the frequencies and buckling loads of a bidirectional varied

Received: June 2022, Accepted: October 2022
Correspondence to: Hareram Lohar
Asst. Prof., Department of Mechanical Engineering
Jadavpur University, Kolkata-700032, India
E-mail: hareraml.mech@jadavpuruniversity.in
doi: 10.5937/fme2204643L

FG thick beam system under the action of axial load, considering Hamilton's principle. Babaei et al. [18] conducted dynamic analysis on a curved FGM beam (arch) to determine loaded/unloaded vibrational frequencies. Fallah and Aghdam [19-20] carried out a large amplitude dynamic and thermo-mechanical stability study on FG beams. Calim [21] studied the dynamic behavior of AFG thick beams. Lohar et al. [7, 22] performed large amplitude dynamic analysis on AFG non-uniform thin and thick beams utilizing Hamilton's principle. Trabelssi et al. [23] investigated the dynamics of a nonlocal thick FG nanobeam to obtain the free vibrational frequencies and frequency-dependent responses of the system. Mohamed et al. [24] considered a numerical analysis to predict curved beams' large amplitude dynamic behavior. Akgöz and Civalek [25], with the help of the strain gradient elasticity technique, studied the flexural stability of FG microbeams. Fazzolari [26] utilized various generalized theories to investigate the critical buckling behavior and force-free vibrational behavior of three-dimensional spongy FG sandwich beams.

Research articles found in the existing literature on structural elements placed on the variable elastic foundation are limited in number. Zhang et al. [27] conducted buckling stability and vibrational frequency analysis on a tapered beam utilizing Hencky bar-chain technique. Kacar et al. [28] predicted the dynamic behavior of a homogeneous beam with the help of the differential transform method. Eisenberger and Clastornik [29] investigated the buckling and vibration characteristics of a homogeneous beam. Mirzabeigy and Madoliat [30] predicted the loaded free vibrational response of an axially loaded beam. Yas et al. [31] introduced the generalized differential quadrature method to observe the free vibrational characteristics of the FGM beam. Kumar [32] utilized the Rayleigh-Ritz principle to predict the vibrational frequency of the AFG beam.

From the literature survey, it is observed that a substantial amount of research articles is present in the literature in which various aspects of FG beam placed on the elastic foundation are explored. But the domain of variable elastic foundation is relatively newer, and a limited number of research works are found in this domain. The problem involves variable foundation, which is more realistic and general as most of the foundations practically behave in a non-homogeneous and anisotropic manner. On the other hand, axially functionally graded (AFG) material has gained popularity as an important material in designing cantilever and rotating components such as turbine and helicopter rotor blades, spacecraft with flexible appendages, etc. [33]. AFG material can be useful in the chemical industry to design the connecting pipe between two chemical containers maintained at a high thermal gradient. To enhance the thermal dissipation rate pin fin's geometry is often tapered. AFG material can be utilized to design such elements to maintain desired conductivity and strength along its length [34]. So, from an application point of view investigation of the domain is needed. Thus, the present study is conducted on an AFG taper beam supported on a variable elastic foundation to investigate the nonlinear free vibration behavior. It is also to be mentioned that backbone curves for the system have been generated in the present paper, which has yet to be reported in the existing literature.

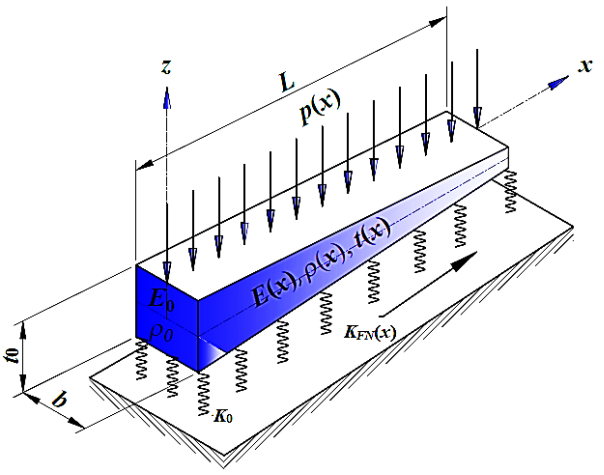

Figure 1. Non-uniform AFG beam model with variable foundation and loading.

2. MATHEMATICAL FORMULATION

Figure 1 represents an AFG beam with tapered geometry of dimensions length L, width b, and non-uniform thickness $t(x)$, resting on variable foundation $K_{FN}(x)$. The linear thickness profile of the beam is selected in which thickness changes along the x-axis,

$$t(x) = t_0\left(1-\alpha\left(\frac{x}{L}\right)\right)$$

The beam taper parameter (α) is used here to adjust the tapering. It is to be observed that the thickness is gradually decreasing from the root side (t_0) to the other side. The smooth transition of modulus of elasticity $E(x)$ and material density $\rho(x)$ in the AFG beam is considered in the axial direction following the power-law relations,

$$E(x) = E_0 + (E_1 - E_0)\left(\frac{x}{L}\right)^n$$

$$\rho(x) = \rho_0 + (\rho_1 - \rho_0)\left(\frac{x}{L}\right)^n$$

Here, n is the gradient index which controls the volume fraction of both constituents involved. E_0 and ρ_0 are the property values at the root ($x = 0$), whereas E_1 and ρ_1 are the corresponding values at the other end of the beam. The foundation is modeled considering a sequential parallel arrangement of linear helical springs connected at the bottommost layer of the beam. The springs are of variable stiffness values, and the variation is considered along the axial direction,

$$K_{FN}(x) = K_0\left(1-\beta\left(\frac{x}{L}\right)\right)$$

here, K_0 is root side stiffness, and β is the stiffness variation parameter.

A displacement-based semi-analytical type of formulation, which is executed in a normalized domain, is

used to mathematically represent the present system. Determination of loaded vibrational frequencies is carried out by considering two well-defined steps. In the first step, the static part is solved under external load, which predicts the initial deflected shape of the beam. In the following step, a dynamic analysis is conducted on the statically deformed system to predict the loaded vibrational frequency. Both static and vibration analysis utilize the suitable principle of energy methods to formulate the governing differential equations. The solution of the governing nonlinear differential equations in matrix form is carried out by the consideration of an appropriate numerical technique.

For simplicity, the beam is selected as 'Euler-Bernoulli's beam', in which thickness is considerably smaller than other dimensions. Hence, the influences of rotational inertia and shearing deformation are negligible. The present study considers the stretching deformation of the beam along with the bending deformation under large amplitude loading. Hence, the strain-displacement relation for bending (ε_{xx}^{b}) and stretching (ε_{xx}^{s}) can be expressed as,

$$\varepsilon_{xx}^{b} = -z\left(\frac{d^2w}{dx^2}\right) \tag{1a}$$

$$\varepsilon_{xx}^{s} = \left(\frac{du}{dx}\right) + \frac{1}{2}\left(\frac{dw}{dx}\right)^2 \tag{1b}$$

Equation (1b) clearly shows nonlinear relation between strain and displacement, which furthermore results in nonlinear governing equations.

The strain energy of the whole system has two separate terms. The first one (I) is due to beam deflection, and another one (II) is due to the presence of a foundation. So total strain energy (U),

$$U = \left[\frac{1}{2}\int_{vol} E(x)\left(\varepsilon_{xx}^{b}\right)^2 dv + \frac{1}{2}\int_{vol} E(x)\left(\varepsilon_{xx}^{s}\right)^2 dv\right]_{\mathrm{I}} \left[+\frac{1}{2}\int_0^L K_f(x) w^2 dx\right]_{\mathrm{II}} \tag{2}$$

Substituting suitable expressions, (2) can be rewritten as

$$U = \frac{1}{2}\int_0^L \left(\frac{d^2w}{dx^2}\right)^2 E(x) I(x) dx + \frac{1}{2}\int_0^L \left[\left(\frac{du}{dx}\right)^2 + \frac{1}{4}\left(\frac{dw}{dx}\right)^4 + \left(\frac{dw}{dx}\right)^2\left(\frac{du}{dx}\right)\right] E(x) A(x) dx + \frac{1}{2}\int_0^L K_f(x) w^2 dx \tag{3}$$

The expression of potential energy (V) under the action of external uniformly distributed load $p(x)$ can be obtained as,

$$V = \int_0^L p(x) w dx \tag{4}$$

Kinetic energy (T) resulting from vibration in the system can be written as,

$$T = \frac{1}{2}\int_0^L \left\{\left(\frac{dw}{d\tau}\right)^2 + \left(\frac{du}{d\tau}\right)^2\right\} \rho(x) A(x) dx \tag{5}$$

The foundation springs are considered massless and hence do not affect the kinetic energy.

Table 1. List of start functions for bending ($w(\xi)$) and stretching ($u(\xi)$) displacement field.

Displacement field	Support Conditions	Start functions
$w(\xi)$	CC	$\phi_1(\xi) = \{\xi(1-\xi)\}^2$
	CS	$\phi_1(\xi) = \xi^2\left(2\xi^2 - 5\xi + 3\right)$
	SS	$\phi_1(\xi) = \sin(\pi\xi)$
	CF	$\phi_1(\xi) = \xi^2\left(\xi^2 - 4\xi + 6\right)$
$u(\xi)$	CC	$\psi_1(\xi) = \xi(1-\xi)$
	CS	
	SS	
	CF	

2.1 Static Analysis

The principle of minimum potential energy is used to formulate the static problem, which follows,

$$\delta(U+V) = 0 \tag{6}$$

The present analysis is a whole domain analysis. To carry out the detailed computation, a suitable number of computational points (which are familiar as gauss points) are created within the normalized domain ($\xi = x/L$). The static displacement fields (w and u) on generated points are assumed following the Rayleigh-Ritz approximation,

$$w(\xi) = \sum_{i=1}^{nw} d_i \phi_i(\xi) \tag{7a}$$

$$u(\xi) = \sum_{i=1+nw}^{nw+nu} d_i \psi_{i-nw}(\xi) \tag{7b}$$

here, d_i are unknown constants. ϕ_i and ψ_i are the functions for w and u, respectively, with orthogonal characteristics. These functions are also said to be admissible as they are selected from satisfying certain conditions. They must be continuous and differentiable in the computation domain and fulfill the kinematic end conditions of the beam. nw and nu are the selected number for these functions ϕ_i and ψ_i, respectively. The first member of these function sets (ϕ_1 and ψ_1) for various end conditions, i.e., CC, SS, CF, and CS, are furnished in Table 1. Here, C, S, and F are clamped, simply-supported and fixed boundaries, respectively. With the help of ϕ_1 and ψ_1, functions up to nw and nu numbers are created by implementing the Gram-Schmidt orthogonalization technique [35]. Substituting equation (3) and equation (4) along with equation (7)

into equation (6), the governing equations of the static problem can be represented in matrix form.

$$[K][d]=\{f\} \tag{8}$$

here, [*K*], {*f*} and {*d*} are stiffness matrix, force vector and vector of unknown parameter, respectively. The de–tailed elements of [*K*] and {*f*} are furnished in the Appendix segment. It can be observed that some ele–ments of [*K*] are a function of the unknown coefficient (d_i). So, a direct solution to the problem is not possible. A numerical scheme of the direct substi–tution method is used to obtain the solution with suitable relaxation parameters [36].

2.2 Dynamic Analysis

The dynamic problem is formulated through the implementation of Hamilton's principle,

$$\delta\left(\int_{\tau_1}^{\tau_2}(T-U)\,d\tau\right)=0 \tag{9}$$

here, τ is the time variable. The expression of U is the same as that of the expression of U in static analysis. The dynamic analysis is carried out on the pre-deformed configuration of the beam, and no external load is applied. Hence, potential energy (V) due to external loading must be zero here.

The dynamic displacement fields w and u are assumed as,

$$w(\xi,\tau)=\sum_{i=1}^{nw} d_i\varphi_i(\xi)e^{i\omega\tau} \tag{10a}$$

$$u(\xi,\tau)=\sum_{i=nw+1}^{nw+nu} d_i\psi_i(\xi)e^{i\omega\tau} \tag{10b}$$

Table 2. Validation of adopted formulation and solution procedure.

BCs	K_f	Natural frequencies ($\sqrt{\omega_1}$)	
		Uniform foundation	Kacar et al. [28]
CC	10	4.7448	4.7535
	100	4.9427	4.9504
SS	10	3.2193	3.2193
	100	3.7484	3.7484
CF	10	2.1745	2.1746
	100	3.2558	3.2558
		Linear Foundation (β = 0.2)	Kacar et al. [28]
CC	10	4.7424	4.7512
	100	4.9219	4.9297
SS	10	3.2118	3.2118
	100	3.6999	3.6999
CF	10	2.1342	2.1343
	100	3.1320	3.1319
		Parabolic Foundation (β = 0.2)	Kacar et al. [28]
CC	10	4.7435	4.7522
	100	4.9314	4.9392
SS	10	3.2150	3.2150
	100	3.7212	3.7212
CF	10	2.1410	2.1410
	100	3.1532	3.1530

The displacement fields in the dynamic analysis are a function of space and time. The former (space) part is the same as that of static analysis. Here, ω indicates the natural frequency of vibration, and d_i represents the eigenvector. Substituting equation (3) and equation (5) along with equation (10) into equation (9), the governing equations of the dynamic analysis can be rewritten in matrix form,

$$-\omega^2[M]\{d\}+[K]\{d\}=0 \tag{11}$$

here, [*M*] represents the mass matrix. The detailed ele–ments of [*M*] are provided in the Appendix. It can be noted that the elements of [*K*] in the dynamic problem are the same as those of the static problem.

3. RESULTS AND DISCUSSIONS

The main objective of the present analysis is to study the effects of variable foundation on loaded natural frequencies of AFG beam. The present study's externally applied load is considered a uniformly distributed load. Alongside the elastic foundation, three different classical supports are selected: CC, SS, and CS. To present the results, the following normalized terms are used for natural frequency (ω) and root foundation stiffness (K_f),

$$\omega=\Omega L^2\sqrt{\frac{\rho_0 A_0}{E_0 I_0}}\;;\; K_f=\frac{K_{FN}L^4}{E_0 I}$$

Four different non-dimensional root stiffness values (K_f) are considered for the variable elastic foundation, which is 0, 10, 10^2, and 10^3, respectively. Four different stiffness variation parameters (β) are also considered to control the foundation stiffness variation, which are 0.0, 0.2, 0.4 and 0.6 respectively. Here, $K_f = 0$ resembles the beam with no foundation, whereas β=0.0 indicates the case of constant elastic foundation. For AFG beam the selected materials are Aluminium (Al) and Zirconia (ZrO_2), having material properties as, Al: E_0 = 70 GPa, ρ_0 = 2702 kg/m^3; ZrO_2: E_1 = 200 GPa, ρ_1 = 5700 kg/m^3. It is to be noted that at the beam's root side (ξ = 0), the material is pure Aluminium. Due to continuous gradation transforms, the material into pure Zirconia at the extreme end (ξ = 1). Four different material gradient parameters (n) are selected, which are 0, 1, 2, and 3, respectively. It is to be noted here that n = 0 indicates homogeneous beam material. To consider the taper effect of the beam geometry four different taper parameters (α) are selected, which are 0.0, 0.2, 0.4, and 0.6, respectively. Here, α = 0.0 indicates the beam with uniform geometry. In the present study geometrical dimensions of the beam are selected as L = 1.0 m, b = 0.02 m and t_0 = 0.005 m.

To carry out a detailed computation a suitable number of orthogonal functions (*nw*/*nu*) and gauss points (*ng*) are to be selected. Improper selection of these parameters may adversely affect the outcomes. So, a suitable convergence study is of utmost importance to select the correct values of these parameters. After performing a suitable convergence study, these values are chosen as *ng* =24 and *nw*= 8.

To justify the present methodology's appropriateness the present article's generated results are compared with the results of a published article by Kacar et al. [28]. For that purpose, the present system is reduced to an equivalent system of the published article to generate the results. The results are tabulated in Table 2. The table shows that the results match satisfactorily.

Non-dimensional natural frequencies of the first two modes are furnished in Table 3 for different combinations of root foundation stiffness (K_f), stiffness variation parameters (β), and material grada–tion index (n). The beam is selected as linear taper with $\alpha = 0.5$. From the table, it can be observed that for all possible combinations, the system's natural frequency increases with an increase in foundation stiffness. But with the increase of stiffness variation parameter, the natural frequency decreases. It can also be noticed that natural frequency increases when the gradation index is varied from 1 to 3. Whereas at $n = 0$, the natural frequency attains its maximum value. The reason is quite understandable that at $n = 0$, the material behaves as a homogeneous material, which is Zirconia. The high density of zirconia results in high natural frequency. Among all the support conditions, the highest value of natural frequency is observed for the CC beam, whereas the lowest value is for the SS beam. This happens due to the rigidity concern of the support ends.

The variation in backbone curves for different values of root foundation stiffness (K_f) is shown in Figure 2 for various support conditions. Four non-dimensional root foundation stiffness values are selected, which are varied from 0 to 103. For all cases, the taper parameter, stiffness variation parameter, and gradation index are kept constant, which are 0.5, 0.5, and 1, respectively. For all cases, it is found that the slope of the backbone curve increases with the increase in root foundation stiffness, which clearly indicates that the system is exhibiting a hardening type of nonlinearity. It can also be observed that curves are close to each other in the case of the CC beam (Figure 2(a)), but for the SS beam (Figure 2(c)), curves are relatively widely spaced.

The variation in backbone curves for different values of stiffness variation parameter (β) is shown in Figure 3 for various support conditions. To generate the plots, the taper parameter, gradation index, and root foundation are kept constant, which are 0.5, 1, and 10^2, respectively.

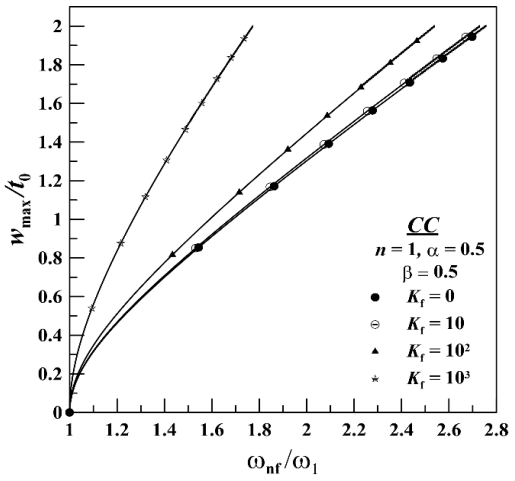

(a)

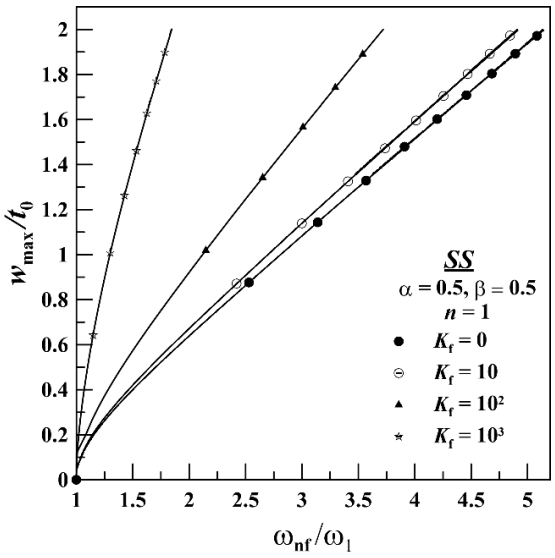

(b)

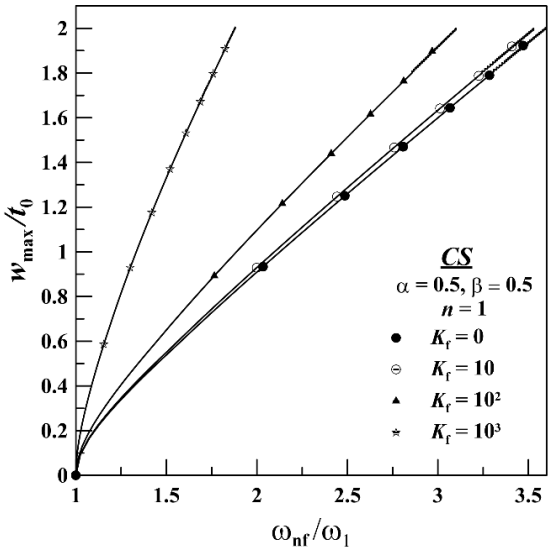

(c)

Figure 2. Backbone curves for different values of root foundation stiffness for (a) CC beam, (b) CS beam, (c) SS beam

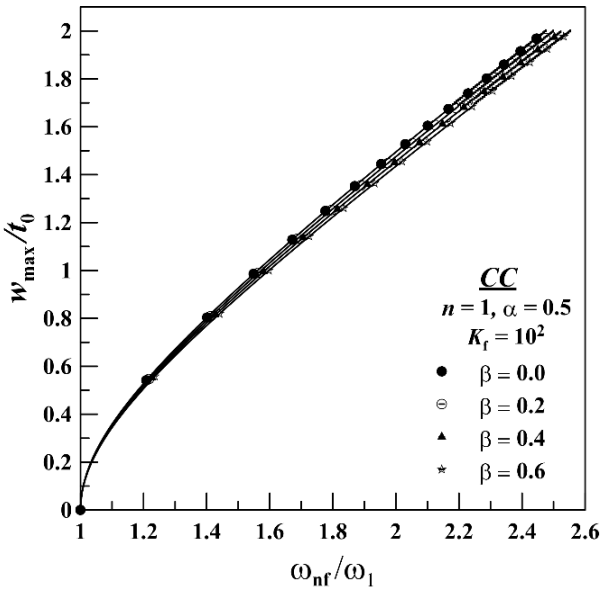

(a)

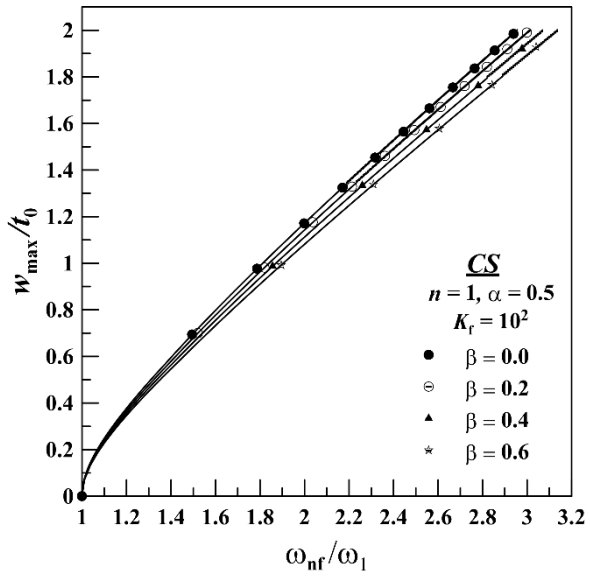

(b)

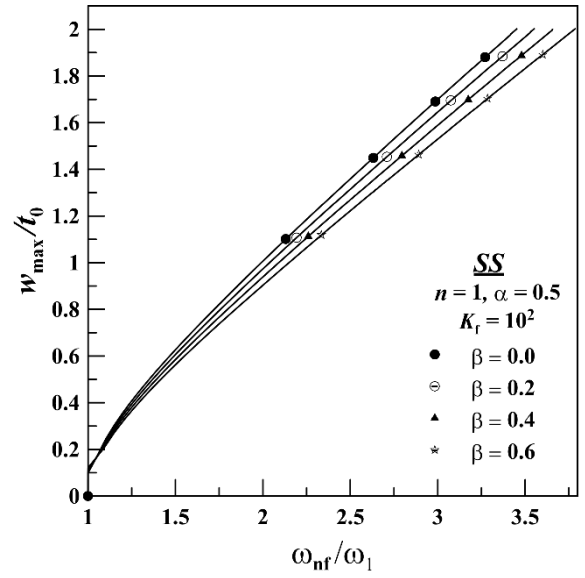

(c)

Figure 3. Backbone curves for different values of stiffness variation parameter for (a) CC beam, (b) CS beam, (c) SS beam.

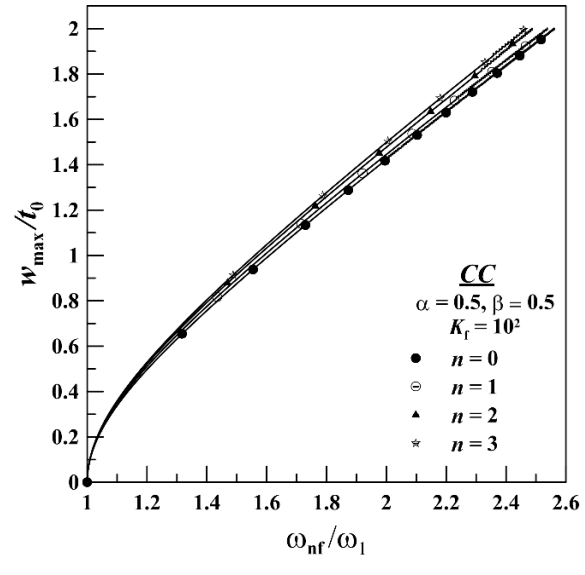

(a)

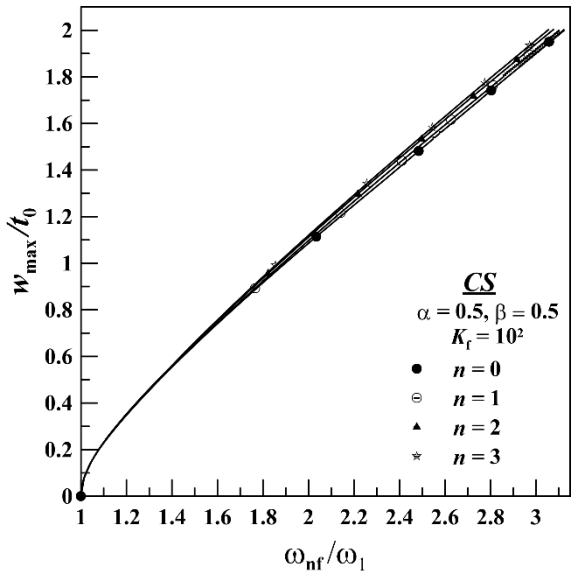

(b)

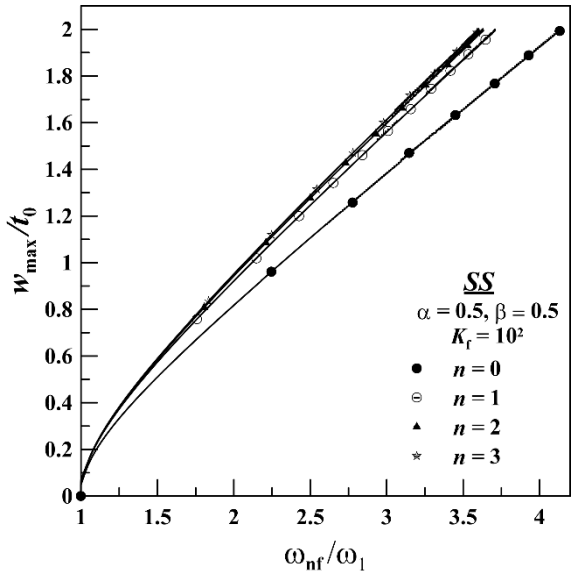

(c)

Figure 4. Backbone curves for different values of material gradation index for (a) CC beam, (b) CS beam, (c) SS beam.

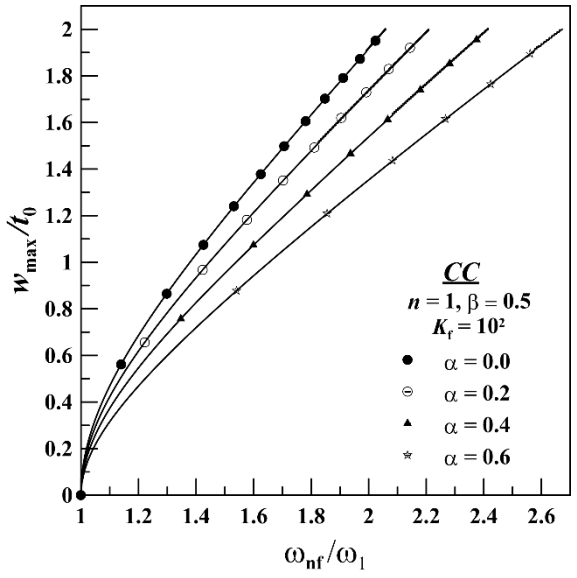

(a)

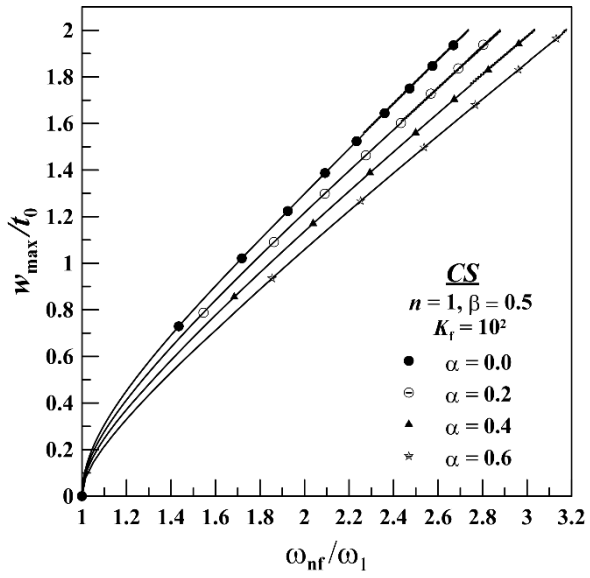

(b)

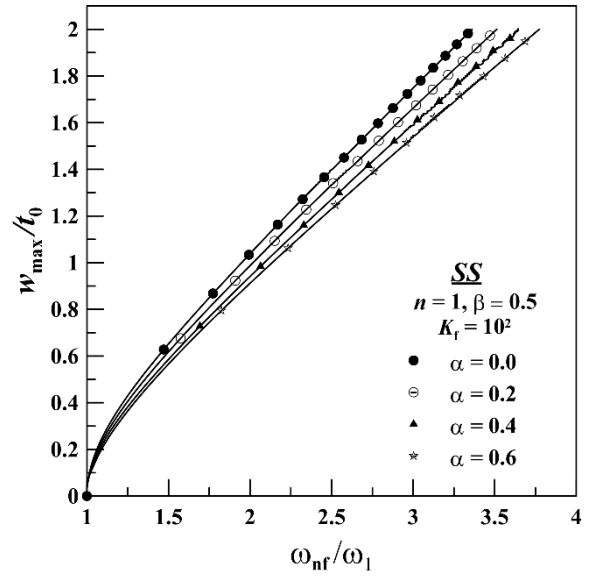

(c)

Figure 5. Backbone curves for different values of taper parameter for (a) CC beam, (b) CS beam, (c) SS beam.

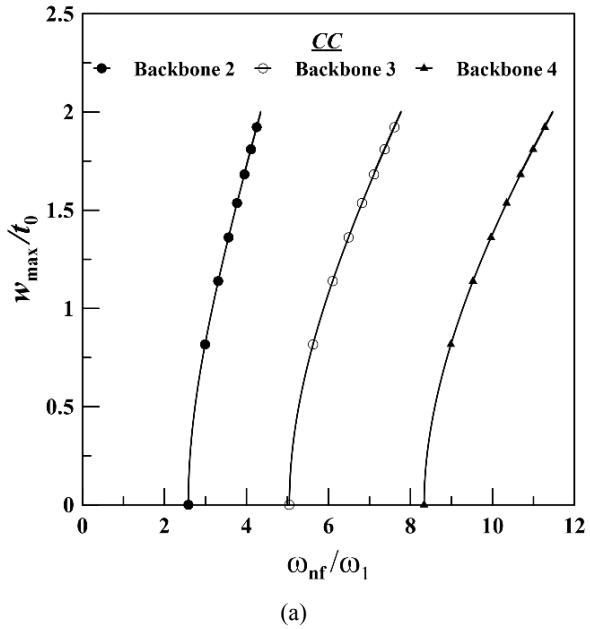

(a)

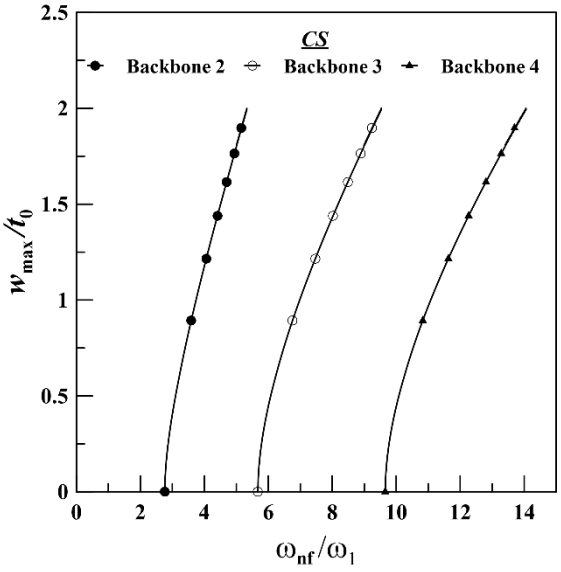

(b)

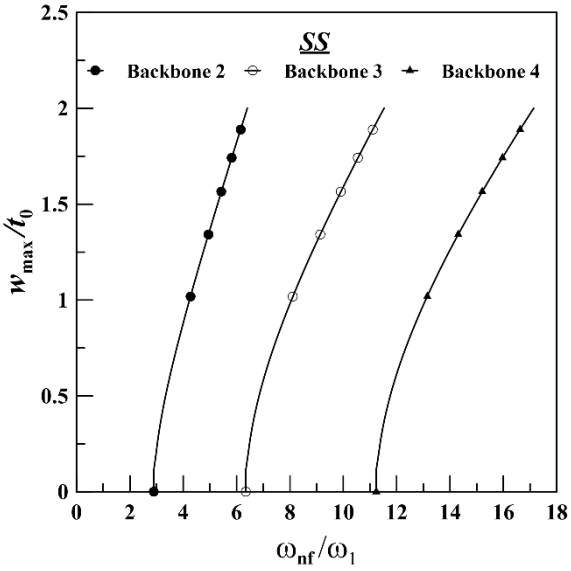

(c)

Figure 6. Higher order backbone curve of (a) CC beam, (b) CS beam, (c) SS beam.

Four stiffness variation parameters are considered, which are selected as 0.0, 0.2, 0.4 and 0.6. For all cases, it is observed that the increment of the stiffness variation parameter results in decrements in the slope of the backbone curve. This type of trend is quite expected from the adopted variable foundation model, in which foundation stiffness gradually decreases from the root side. The stiffness variation parameter's increased value results in more foundation stiffness decrement. As a result, the slope of the backbone curves further decreases.

The variation in backbone curves for different values of material gradation index (n) is shown in Figure 4 for various support conditions. To generate the plots, the taper parameter, root foundation stiffness, and stiffness variation parameter are kept constant, which are 0.5, 10^2, and 0.5, respectively. Four gradation indexes are considered, which are selected as 0, 1, 2, and 3. For all cases, the increasing slope pattern in the backbone curve is observed with the increment of the gradation index.

Table 3. Effect of foundation stiffness (K_f), stiffness variation parameter (β), and material gradation index (n) on the natural frequency of the system, CC, and CS boundary conditions.

K_f	β	n							
		0		1		2		3	
		$\sqrt{\omega_1}$	$\sqrt{\omega_2}$	$\sqrt{\omega_1}$	$\sqrt{\omega_2}$	$\sqrt{\omega_1}$	$\sqrt{\omega_2}$	$\sqrt{\omega_1}$	$\sqrt{\omega_2}$
CC									
0	-	4.3519	7.2201	4.1684	6.9787	4.2005	6.9572	4.2257	6.9441
10	0	4.3716	7.2245	4.1980	6.9852	4.2349	6.9648	4.2632	6.9524
	0.2	4.3695	7.2240	4.1949	6.9845	4.2313	6.9640	4.2592	6.9515
	0.4	4.3673	7.2235	4.1918	6.9838	4.2277	6.9632	4.2553	6.9507
	0.6	4.3651	7.2230	4.1887	6.9831	4.2241	6.9625	4.2514	6.9498
100	0	4.5384	7.2638	4.4397	7.0425	4.5122	7.0322	4.5626	7.0259
	0.2	4.5189	7.2588	4.4132	7.0359	4.4822	7.0245	4.5303	7.0175
	0.4	4.4991	7.2539	4.3863	7.0293	4.4515	7.0169	4.4974	7.0091
	0.6	4.4790	7.2489	4.3888	7.0226	4.4202	7.0092	4.4636	7.0007
1000	0	5.6410	7.6258	5.8459	7.5513	6.0537	7.6188	6.1851	7.6587
	0.2	5.5387	7.5824	5.7270	7.4972	5.9255	7.5585	6.0518	7.5937
	0.4	5.4294	7.5384	5.5993	7.4421	5.7875	7.4969	5.9079	7.5272
	0.6	5.3121	7.4939	5.4612	7.3859	5.6378	7.4341	5.7514	7.4593
CS									
0	-	3.7801	6.6028	3.5512	6.3434	3.5460	6.3050	3.5485	6.2755
10	0	3.8114	6.6086	3.5987	6.3520	3.6018	6.3152	3.6101	6.2867
	0.2	3.8076	6.6079	3.5932	6.3510	3.5954	6.3141	3.6030	6.2854
	0.4	3.8038	6.6072	3.5877	6.3501	3.5889	6.3130	3.5958	6.2843
	0.6	3.7999	6.6065	3.5821	6.3492	3.5823	6.3119	3.5886	6.2832
100	0	4.0628	6.6606	3.3597	6.4208	4.0157	6.4048	4.0592	6.3849
	0.2	4.0313	6.6538	3.9177	6.4189	3.9683	6.3943	4.0081	6.3735
	0.4	3.9991	6.6470	3.8744	6.4098	3.9191	6.3838	3.9549	6.3620
	0.6	3.9660	6.6401	3.8295	6.4006	3.8679	6.3733	3.8994	6.3505
1000	0	5.4524	7.1254	5.6609	7.0717	5.8569	7.1441	5.9895	7.1823
	0.2	5.3222	7.0682	5.5135	7.0027	5.6986	7.0687	5.8245	7.1019
	0.4	5.1798	7.0101	5.3515	6.9320	5.5241	6.9913	5.6423	7.0192
	0.6	5.0224	6.9511	5.1713	6.8597	5.3296	6.9116	5.4385	6.9341
SS									
0	-	2.8789	5.8043	2.8391	5.6551	2.7939	5.5690	2.7612	5.5227
10	0	2.9443	5.8128	2.9298	5.6674	2.9073	5.5837	2.8872	5.5389
	0.2	2.9375	5.8118	2.9208	5.6661	2.8944	5.5822	2.8749	5.5372
	0.4	2.9307	5.8109	2.9117	5.6648	2.8834	5.5807	2.8625	5.5356
	0.6	2.9239	5.8099	2.9025	5.6635	2.8722	5.5792	2.8499	5.5339
100	0	3.3975	5.8810	3.5114	5.7739	3.5790	5.7113	3.6197	5.6791
	0.2	3.3530	5.8785	3.4580	5.7618	3.5194	5.6972	3.5562	5.6634
	0.4	3.3065	5.8688	3.4018	5.7497	3.4564	5.6830	3.4888	5.6477
	0.6	3.2578	5.8591	3.3425	5.7374	3.3896	5.6688	3.4171	5.6319
1000	0	5.1601	6.5215	5.5305	6.6106	5.7477	6.6743	5.8770	6.7121
	0.2	5.0373	6.4474	5.3897	6.5294	5.5973	6.5866	5.7227	6.6180
	0.4	4.9009	6.3718	5.2334	6.4464	5.4298	6.4969	5.5498	6.5219
	0.6	4.7476	6.2948	5.0578	6.3614	5.2410	6.4049	5.3538	6.4236

Backbone curves generated from different values of taper parameters (α) are shown in Figure 5. To generate the plots root foundation stiffness, stiffness variation parameter, and gradation index are kept constant, which are 10^2, 0.5, and 1, respectively.

Four taper parameters are considered, which are selected as 0.0, 0.2, 0.4 and 0.6. For all cases, the figure shows that the slope of the backbone curve is reduced by the increased value of the taper parameter. These results can be justified by the adopted taper pattern, in which the thickness of the beam gradually decreases from the root side to the other ends. Furthermore, the increased value of the taper parameter decreases the overall volume of the beam, which implies a decrement in the total mass of the beam system. As a result, the above-mentioned trend is found.

Higher mode backbone curves are also important for the nonlinear analysis of the continuous system. The amount of nonlinearity involved at higher mode can be predicted from these plots. Backbone curves for modes 2-4 corresponding to four different boundary conditions are shown in Figure 6. To generate the results root foundation stiffness, stiffness variation parameter, gradation index, and taper parameter are kept constant, which are 10^2, 0.5, 1, and 0.5 respectively. It is to be noted that backbone curves beyond mode 4 are also possible to represent. But those curves are not shown here to maintain the clarity of the plots.

The first three mode shapes for three various support conditions are shown in Figure 7. For each vibration mode, two distinct mode shapes are shown. One is a linear mode shape, obtained at no load condition

($w_{max}/t_0 = 0$), and another one is a nonlinear mode shape, obtained at loaded condition ($w_{max}/t_0 = 2$). The difference between these two measures the amount of nonlinearity present in the system. To generate the results root foundation stiffness, stiffness variation parameter, gradation index, and taper parameter are kept constant, which are 10^2, 0.5, 1, and 0.5, respectively.

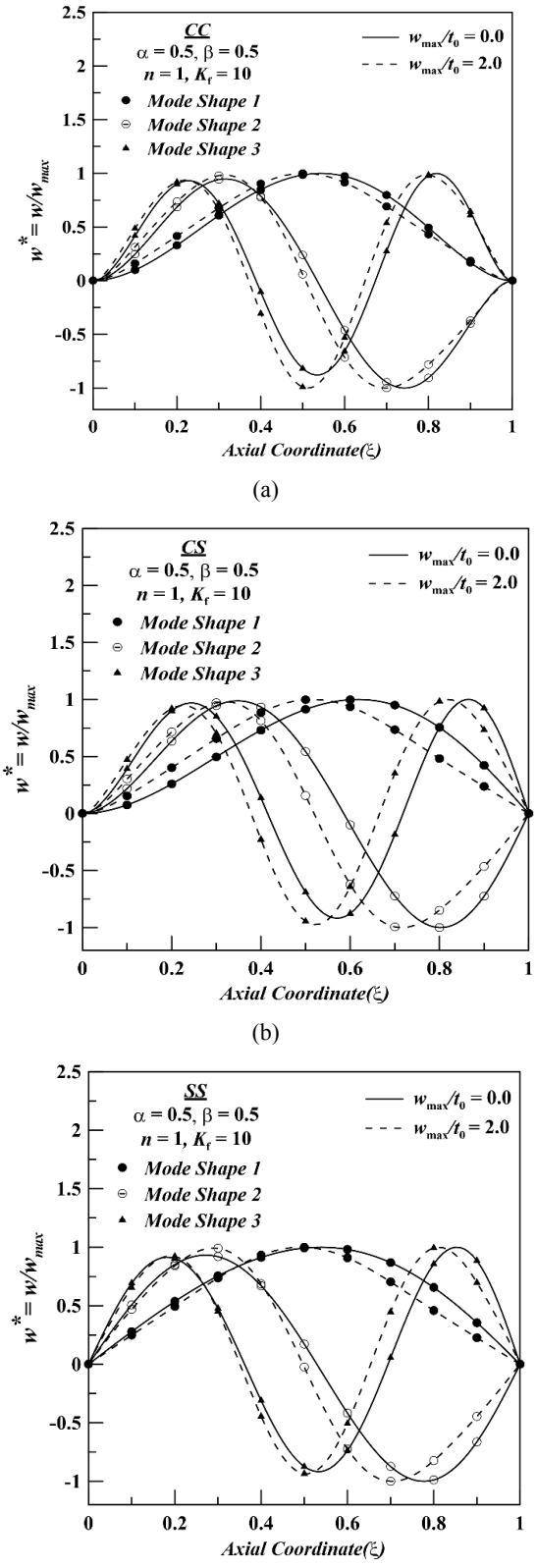

Figure 7. First three Linear and nonlinear mode shapes of (a) CC beam, (b) CS beam, (c) SS beam.

4. CONCLUSIONS

The present study is carried out on a tapered AFG beam to determine the effect of variable foundation on the large amplitude free vibrational behavior of the system. Geometric nonlinear type of system behavior is introduced into the present formulation through the consideration of higher order nonlinear terms in strain-displacement relation. The axial gradation of the beam material is considered to follow the power law expression. A variable Winkler type of elastic foundation is introduced in the present system. Whole domain analysis is performed in a normalized coordinate system, which is formulated by the Rayleigh-Ritz principle and solved by using a numerical tool. The adopted methodology is validated with the results of existing literature. Benchmark results are also obtained in terms of natural frequency, backbone curve, and mode shape plot for a different set of parameters which are considered in the present study.

The key outcomes of the study can be summarized as,

- For all possible combinations, the natural frequency of the system increases with an increase in foundation stiffness. But with the increase of stiffness variation parameter, the natural frequency decreases.
- It can also be noticed that natural frequency inc–reases when the gradation index is varied from 1 to 3.
- Among all the support conditions, the highest value of natural frequency is observed for the CC beam, whereas the lowest value is for the SS beam.
- It is observed that the system shows a hardening type of nonlinear behavior under large amplitude loading.
- For all possible combinations, it is noticed that the slope of the backbone curve increases with the increase of root foundation stiffness, whereas the increment of stiffness variation parameter results in decrements in the slope of the backbone curve.

APPENDIX

The elements of [K] are,

$$\left[K_{ij}\right]_{\substack{i=1,nw\\ j=1,nw}} = \frac{1}{L^3}\int_0^1 \frac{d^2\phi_i}{d\xi^2}\frac{d^2\phi_j}{d\xi^2}E(\xi)I(\xi)d\xi +$$

$$\frac{1}{2L^3}\int_0^1\left(\sum_{k=1}^{nw} d_k \frac{d\phi_k}{d\xi}\right)^2 \frac{d\phi_i}{d\xi}\frac{d\phi_j}{d\xi}E(\xi)A(\xi)d\xi$$

$$+\frac{1}{L^2}\int_0^1\left(\sum_{k=1+nw}^{nw+nu} d_k \frac{d\psi_{k-nw}}{d\xi}\right)\frac{d\phi_i}{d\xi}\frac{d\phi_j}{d\xi}E(\xi)A(\xi)d\xi +$$

$$L\int_0^1 \phi_i\phi_j K_f(\xi)d\xi$$

$$\left[K_{ij}\right]_{\substack{i=1,nw\\ j=1+nw,nw+nu}}$$

$$= \frac{1}{2L^2}\int_0^1\left(\sum_{k=1}^{nw} d_k \frac{d\phi_k}{d\xi}\right)\frac{d\phi_i}{d\xi}\frac{d\psi_{j-nw}}{d\xi}E(\xi)A(\xi)d\xi$$

$$\left[K_{ij}\right]_{\substack{i=1+nw,nw+nu \\ j=1,nw}} = 0$$

$$\left[K_{ij}\right]_{\substack{i=1+nw,nu+nw \\ j=1+nw,nu+nw}} = \frac{1}{L}\int_0^1 \frac{d\psi_{i-nw}}{d\xi}\frac{d\psi_{j-nw}}{d\xi}E(\xi)A(\xi)d\xi$$

The elements of $\{f\}$ are,

$$\left\{f_j\right\}_{j=1,nw} = pL\int_0^1 \phi_j d\xi$$

$$\left\{f_j\right\}_{j=1+nw,nw+nu} = 0$$

The elements of $[M]$ are,

$$\left[M_{ij}\right]_{\substack{i=1,nw \\ j=1,nw}} = L\int_0^L \phi_i\phi_j A(\xi)\rho(\xi)d\xi$$

$$\left[M_{ij}\right]_{\substack{i=nw+1,nw+nu \\ j=nw+1,nw+nu}} = L\int_0^L \alpha_{i-nw}\alpha_{j-nw}A(\xi)\rho(\xi)d\xi$$

$$\left[M_{ij}\right]_{\substack{i=nw+nu+1,nw+nu+nsi \\ j=nw+nu+1,nw+nu+nsi}} = L\int_0^L \beta_{i-nw-nu}\beta_{j-nw-nu}I(\xi)\rho(\xi)d\xi$$

NOMENCLATURE

L, b, t	Length, breadth and thickness of the beam geometry, respectively
K_{FN}, K_f	Dimensional and non-dimensional stiffness value of the elastic foundation, respectively
α	Taper parameter of beam geometry
E , ρ	Elastic modulus and density of beam of beam, respectively
n	Material gradation index
t_0	Root thickness of beam
K_0	Root stiffness of the foundation
β	Stiffness variation parameter
E_0 , ρ_0	Root side value of E and ρ, respectively
E_1, ρ_1	E and ρ at the extreme end of beam, respectively
ε_{xx}^b , ε_{xx}^s	Axial strain due to bending and stretching, respectively
w, u	Bending and stretching displacement fields, respectively
U, V, T	Strain energy, potential energy, and kinetic energy, respectively.
A, I	Beam cross-section and area moment of inertia of the beam cross-section about neutral axis, respectively.
A_0, I_0	Root value of A and I, respectively.
δ	Variational operator
d_i	Unknown coefficients
ϕ_i , ψ_i	Set of orthogonal functions for w and u, respectively
ϕ_1 , ψ_1	Start functions for w and u, respectively
Ω, ω	Dimensional and non-dimensional natural frequency
$[K]$	Stiffness matrix
$[M]$	Mass matrix
$\{f\}$	Load vector
$\{d\}$	Vector of unknown co-efficient
τ	Time coordinate
nw, nu	Number of constituent functions for w and u respectively
ng	Number of Gauss points
$p(x)$	Magnitude of uniformly distributed load
w_{max}	Maximum deflection of the beam
ξ	Normalized axial coordinate
ω_1	First natural frequency
ω_{nf}	Nonlinear frequency

ACRONYM LIST

FGM	Functionally Graded Material
AFG	Axially Functionally Graded
BC	Boundary Condition
CC	Clamped-Clamped
CS	Clamped-Simply supported
SS	Simply supported- Simply supported
CF	Clamped-Free

REFERENCE

[1] Koizumi, M.: FGM activities in Japan, Compos. B. Eng., Vol. 28B, pp.1–4, 1997.

[2] Suresh, S. and Mortensen, A.: *Fundamentals of Functionally Graded Materials*, IOM Communi–cations Limited, London, 1998.

[3] Dinulović, M., Rašuo, B., Slavković, A., Zajić, G.: Flutter Analysis of Tapered Composite Fins: Analysis and Experiment, FME Transactions, Vol. 50 (3), pp. 576-585, 2022

[4] Dinulović, M., Rašuo, B., Trninić, MR., Adžić, VM.: Numerical Modeling of Nomex Honeycomb Core Composite Plates at Meso Scale Level, FME Transactions, Vol. 48 (4), pp. 874-881, 2020

[5] Maksimović, K., Maksimović, M., Vasović Maksimović, I., Rašuo, B., Maksimović, S.: Postbuckling and Failure Analysis of Layered Composite Panels, FME Transactions, Vol. 48 (2), pp. 447-453, 2020

[6] Garinis, D., Dinulović, M., Rašuo B.: Dynamic analysis of modified composite helicopter blade, FME Transactions, Vol. 40 (2), pp. 63-68, 2012

[7] Lohar, H., Mitra, A. and Sahoo, S.: Geometric nonlinear free vibration of axially functionally graded non-uniform beams supported on elastic foundation, Curved Layer. Struct., Vol. 3, No. 1, pp. 223–239, 2016.

[8] Pradhan, S.C. and Murmu, T.: Thermo-mechanical vibration of FGM sandwich beam under variable elastic foundations using differential quadrature method, J. Sound Vib., Vol. 321, pp. 342–362, 2009.

[9] Attar, M., Karrech, A. and Regenauer-Lieb, K.: Free vibration analysis of a cracked shear deformable beam on a two-parameter elastic foundation using a lattice spring model, J. Sound Vib., Vol. 333, pp. 2359–2377, 2014.

[10] Yaghoobi, H. and Torabi, M.: Post-buckling and nonlinear free vibration analysis of geometrically

imperfect functionally graded beams resting on nonlinear elastic foundation, Appl. Math. Model., Vol. 37, pp.8324–8340, 2013.

[11] Mohanty, S.C., Dash, R.R. and Rout, T.: Parametric instability of a functionally graded Timoshenko beam on Winkler's elastic foundation, Nucl. Eng. Des., Vol. 241, pp. 2698– 2715, 2011.

[12] Murin, J., Aminbaghai, M., Kutis, V. and Hrabovsky, J.: Modal analysis of the FGM beams with effect of axial force under longitudinal variable elastic Winkler foundation, Eng. Struct., Vol. 49, pp. 234–247, 2013.

[13] Mohanty, M., Pramanik, S. K. and Pradhan, M.: Analysis of dynamic stability of a tapered two layer elastic beam resting on a variable Pasternak foundation subjected to axial pulsating load, Materials Today: Proceedings, Vol. 46, pp. 4464–4469, 2021.

[14] Kanani, A.S., Niknam, H., Ohadi, A.R. and Aghdam, M.M.: Effect of nonlinear elastic foundation on large amplitude free and forced vibration of functionally graded beam, Compos. Struct., Vol. 115, pp. 60–68, 2014.

[15] Niknam, H. and Aghdam, M.M.: A semi analytical approach for large amplitude free vibration and buckling of nonlocal FG beams resting on elastic foundation, Compos. Struct., Vol. 119, pp. 452–462, 2015.

[16] Tossapanon, P. and Wattanasakulpong, N.: Stability and free vibration of functionally graded sandwich beams resting on two-parameter elastic foundation, Compos. Struct., Vol. 142, pp. 215–225, 2016.

[17] Deng, H., Chen, K., Cheng, W. and Zhao, S.: Vibration and buckling analysis of double-functionally graded Timoshenko beam system on Winkler-Pasternak elastic foundation, Compos. Struct., Vol. 160, pp. 152–168, 2017.

[18] Babaei, H., Kiani, Y., Eslami, M.R.: Large amplitude free vibration analysis of shear deformable FGM shallow arches on nonlinear elastic foundation, Thin-Walled Struct., Vol. 144, pp.106-237, 2019.

[19] Fallah, A. and Aghdam, M.: Nonlinear free vibration and post-buckling analysis of functionally graded beams on nonlinear elastic foundation, Eur J Mech A Solids, Vol. 30, pp. 571-583, 2011.

[20] Fallah, A. and Aghdam, M.: Thermo-mechanical buckling and nonlinear free vibration analysis of functionally graded beams on nonlinear elastic foundation, Compos. B. Eng., Vol. 43, pp. 1523–1530, 2012.

[21] Calim, F.F.: Free and forced vibration analysis of axially functionally graded Timoshenko beams on two-parameter viscoelastic foundation, Compos. B. Eng., Vol. 103, pp. 98-112, 2016.

[22] Lohar, H., Mitra, A. and Sahoo, S.: Large amplitude forced vibration analysis of an axially functionally graded tapered beam resting on elastic foundation, Materials Today: Proceedings, Vol. 5, No. 2, pp. 5303–5312, 2018.

[23] Trabelssi, M., Borgi, S.E., Fernandes, R. and Ke, L.L.: Nonlocal free and forced vibration of a graded Timoshenko nanobeam resting on a nonlinear elastic foundation, Compos. B. Eng., Vol. 157, pp. 331–349. 2019.

[24] Mohamed, N., Eltaher, M.A., Mohamed, S.A. and Seddek, L.F.: Numerical analysis of nonlinear free and forced vibrations of buckled curved beams resting on nonlinear elastic foundations, Int. J. Non-Linear Mech., Vol. 101, pp. 157–173, 2018.

[25] Akgöz, B. and Civalek, O.: Bending analysis of FG microbeams resting on Winkler elastic foundation via strain gradient elasticity, Compos. Struct., Vol. 134, pp. 294–301, 2015.

[26] Fazzolari, F.A.: Generalized exponential, polynomial and trigonometric theories for vibration and stability analysis of porous FG sandwich beams resting on elastic foundations, Compos. B. Eng., Vol. 136, pp. 254–271, 2018.

[27] Zhang, H., Wang, C.M., Ruocco, E. and Challamel, N.: Hencky bar-chain model for buckling and vibration analyses of non-uniform beams on variable elastic foundation, Eng. Struct., Vol.126, pp. 252-263, 2016.

[28] Kacar, A., Tan, H.T. and Kaya, M.O.: Free vibration analysis of beams on variable Winkler elastic foundation by using the differential transform method, Math. Comput. Appl., Vol. 16, No. 3, pp. 773–783, 2011.

[29] Eisenberger, M. and Clastornik, J.: Vibrations and buckling of a beam on a variable Winkler elastic foundation, J. Sound Vib., Vol. 115, No. 2, pp. 233–241, 1987.

[30] Mirzabeigy, A. and Madoliat, R.: Large amplitude free vibration of axially loaded beams resting on variable elastic foundation, Alex. Eng. J., Vol. 55, No. 2, pp. 1107–1114, 2016.

[31] Yas, M.H., Kamarian, S. and Pourasghar, A.: Free vibration analysis of functionally graded beams resting on variable elastic foundations using a generalized power-law distribution and GDQ method, Ann. Solid Struct. Mech., Vol. 9, No. 1-2, pp. 1–11, 2017.

[32] Kumar, S.: Dynamic behaviour of axially functionally graded beam resting on variable elastic foundation, Arch. Mech. Eng., Vol. 67, No. 4, pp. 451-470, 2020.

[33] Bera, S., Lohar, H. and Mitra, A.: Free vibration of axially graded Timoshenko beam under centrifugal stiffening, AIP Conference Proceedings 2200, pp. 020020-1- 020020-10, 2019. https://doi.org/10.1063/1.5141190

[34] Sahu, A. and Bhowmick, S.: Numerical investigation of transient responses of triangular fins having linear and power law property variation under step changes in base temperature and base heat flux using lattice Boltzmann method, Numer. Heat Transf. A: Appl, Vol. 80, pp. 234-254, 2021.

[35] Kumar, S., Mitra, A. and Roy, H.: Geometrically nonlinear free vibration analysis of axially

functionally graded taper beams, Int. J. Eng. Sci. Technol., Vol. 18, pp. 579-593, 2015.

[36] Lohar, H., Mitra, A. and Sahoo, S.: Natural frequency and mode shapes of exponential tapered AFG beams on elastic Foundation, International Frontier Science Letters, Vol. 9, pp. 09-25, 2016.

АНАЛИЗА НЕЛИНЕАРНИХ СЛОБОДНИХ ВИБРАЦИЈА НЕУЈЕДНАЧЕНЕ АКСИЈАЛНО СТЕПЕНОВАНЕ ГРЕДЕ НА ПРОМЕНЉИВОЈ ЕЛАСТИЧНОЈ ОСНОВИ

Х. Лохар, А. Митра

Овај рад истражује нелинеарне слободне вибрације аксијално функционално степеноване (АФГ) греде ослоњене на променљиву основу. Геометрија греде је неуједначена, са линеарном варијацијом попречног пресека по дужини. Материјал греде се степенује дуж аксијалног правца пратећи однос степена и закона. Узима се Винклер тип променљиве еластичне основе, у коме се разматра варијација крутости по дужини темеља. Такође је узета у обзир геометријска нелинеарност изазвана скретањем греде велике амплитуде. Да би се постигли жељени циљеви, проблем је подељен на два дела.

Прво се решава статички проблем, а затим се врши накнадна анализа слободних вибрација на статички деформисаној конфигурацији греде. Водеће диференцијалне једначине система су изведене коришћењем одговарајућих енергетских метода. Нумеричка техника директне замене са релаксацијом се користи за добијање решења изведених нелинеарних диференцијалних једначина. Представљена је одговарајућа студија валидације како би се осигурала прикладност садашње методологије. Резултати бенчмарка су такође представљени помоћу природне фреквенције, криве кичме и дијаграма облика облика да би се истражили утицаји еластичне основе, градације материјала и неуједначене геометрије на нелинеарне вибрације.